Science of the Total Environment 538 (2015) 789–801

Contents lists available at ScienceDirect

Science of the Total Environment

journal homepage: www.elsevier.com/locate/scitotenv

Modeling long-term uptake and re-volatilization of semi-volatile organic compounds (SVOCs) across the soil–atmosphere interface

Zhongwen Bao [a,*], Christina Haberer [a], Uli Maier [b], Barbara Beckingham [c], Richard T. Amos [d], Peter Grathwohl [a]

[a] University of Tübingen, Department of Geosciences, Hölderlinstr. 12, 72074 Tübingen, Germany
[b] Helmholtz Center for Environmental Research — UFZ, Department of Hydrogeology, Permoserstr. 15, 04318 Leipzig, Germany
[c] College of Charleston, Department of Geology and Environmental Geosciences, 202 Calhoun Street, 29401 Charleston, SC, United States
[d] Carleton University, Department of Earth Sciences, 1125 Colonel By Drive, K1S 5B6 Ottawa, ON, Canada

HIGHLIGHTS

- Coupling of soil and the atmosphere in numerical model (MIN3P).
- Long-term soil-atmosphere exchange of SVOCs is controlled by the soil.
- Reduction of atmospheric pollution leads to short-term re-volatilization of pollutants.
- On the long term soils generally are sinks for atmospheric pollutants.

GRAPHICAL ABSTRACT

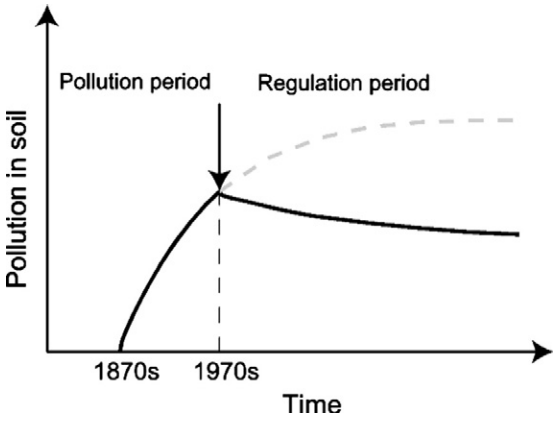

ARTICLE INFO

Article history:
Received 17 May 2015
Received in revised form 22 July 2015
Accepted 17 August 2015
Available online 1 September 2015

Editor: D. Barcelo

Keywords:
Soil and atmosphere pollution
Diffusion
Sorption
Biodegradation
Groundwater recharge
Phenanthrene

ABSTRACT

Soil–atmosphere exchange is important for the environmental fate and atmospheric transport of many semi-volatile organic compounds (SVOCs). This study focuses on modeling the vapor phase exchange of semi-volatile hydrophobic organic pollutants between soil and the atmosphere using the multicomponent reactive transport code MIN3P. MIN3P is typically applied to simulate aqueous and vapor phase transport and reaction processes in the subsurface. We extended the code to also include an atmospheric boundary layer where eddy diffusion takes place. The relevant processes and parameters affecting soil–atmosphere exchange were investigated in several 1-D model scenarios and at various time scales (from years to centuries). Phenanthrene was chosen as a model compound, but results apply for other hydrophobic organic compounds as well. Gaseous phenanthrene was assumed to be constantly supplied to the system during a pollution period and a subsequent regulation period (with a 50% decline in the emission rate). Our results indicate that long-term soil–atmosphere exchange of phenanthrene is controlled by the soil compartment — re-volatilization thus depends on soil properties. A sensitivity analysis showed that accumulation and transport in soils in the short term is dominated by diffusion, whereas in the long term groundwater recharge and biodegradation become relevant. As expected, sorption causes retardation and slows down transport and biodegradation. If

* Corresponding author.
E-mail address: zhongwen.bao@uni-tuebingen.de (Z. Bao).

http://dx.doi.org/10.1016/j.scitotenv.2015.08.104

atmospheric concentration is reduced (e.g. after environmental regulations), re-volatilization from soil to the atmosphere occurs only for a relatively short time period. Therefore, the model results demonstrate that soils generally are sinks for atmospheric pollutants. The atmospheric boundary layer is only relevant for time scales of less than one month. The extended MIN3P code can also be applied to simulate fluctuating concentrations in the atmosphere, for instance due to temperature changes in the topsoil.

1. Introduction

Over the last two centuries, many semi-volatile organic compounds (SVOCs), such as organochlorine pesticides, polychlorinated biphenyls (PCBs), and polycyclic aromatic hydrocarbons (PAHs), have been produced and intentionally or unintentionally released to the environment due to various anthropogenic activities. For instance, pesticides have been applied on arable land for agricultural production and are still used in developing countries (e.g. DDT for malaria control), PCBs were and still are released into the atmosphere from PCB-containing buildings, electrical equipment and contaminated sediments (Jamshidi et al., 2007), and PAHs are produced as byproducts in combustion of fossil fuels and biomass burning. SVOCs may persist in the environment due to their affinity to natural organic matter in soils or sediments and if they are resistant to photolytic, chemical, and microbial degradation, and can pose risks to ecosystems and human health due to their inherent toxicity, persistence, and tendency for long-range transport and accumulation in organisms.

Since the beginning of industrialization and agriculture intensification, soils became sinks for many SVOCs, some of which are now considered as legacy pollutants. Once applied or released into the atmosphere, SVOCs are transported regionally or globally by atmospheric cycling (van Jaarsveld et al., 1997; Beyer et al., 2000; Totten et al., 2006; Lohmann et al., 2007). As a consequence of atmospheric transport, deposition and re-volatilization, soils have become contaminated at a large scale (Lang et al., 2007). Yet, environmental legislation and technological progress already in place or on the horizon aim to limit emission or application of certain compounds, thus decreasing atmospheric concentrations. Therefore, soils preloaded with SVOCs now may act as secondary sources and SVOCs may re-volatilize to the atmosphere. Soil–atmosphere exchange, therefore, is a critical process determining the long-range/global transport of many SVOCs (Cousins et al., 1999a).

To evaluate the exchange of SVOCs between soil and the atmosphere, several combined soil–atmosphere models (Reichman et al., 2000a, 2000b; Scholtz and Bidleman, 2006, 2007; Komprda et al., 2013) were developed to specifically describe the environmental fate of surface-applied pesticides as a function of the compound's volatilization rate. In contrast, only few studies have focused on the numerical evaluation of soil–atmosphere exchange of global pollutants such as PAHs and PCBs (Harner et al., 1995; Lee et al., 1998; Wania and Dugani, 2003; Wania et al., 2006; Mackay, 2010; Ghirardello et al., 2010), and even fewer studies investigated the vertical concentration distributions of PAHs and PCBs in soil and the atmosphere (Cousins et al., 1999b, 1999c; Moeckel et al., 2009). Whereas soil–atmosphere exchange has been studied in the field at time scales from hours to seasons (Lee et al., 1998; Bidleman and Leone, 2004; Lang et al., 2007; Tao et al., 2007, 2008; Bozlaker et al., 2008a, 2008b; Schuster et al., 2010; Cabrerizo et al., 2011; Wang et al., 2011; Zhang et al., 2011; Zhong and Zhu, 2013), detailed long-term simulations on pollutant uptake in soils and re-volatilization – specifically that address the vertical concentration distribution across the soil–atmosphere interface – are missing.

In this study, we extended a numerical model to describe the long-term vapor phase exchange of SVOCs between soil and the atmosphere under varying boundary conditions. Phenanthrene ($C_{14}H_{10}$) was chosen as a model compound and we specifically focused on the vertical concentration profiles across the soil–atmosphere interface. The main objectives of this study were (*i*) to extend a subsurface multicomponent reactive transport code (MIN3P) by considering an atmospheric boundary layer and taking into account the most relevant transport processes (i.e., advective transport with groundwater recharge, sorption, air–water partitioning, biodegradation, and diffusion), (*ii*) to investigate which processes affect soil–atmosphere exchange of SVOCs in the long term and when steady state will be achieved, and (*iii*) to evaluate the re-volatilization potential after regulations limit input of SVOCs into the atmosphere. Focus of our study was not on matching field data but on the theoretical evaluation of the physico-chemical processes in order to identify the most sensitive parameters in long-term uptake and re-volatilization of organic compounds.

2. Background on soil–atmosphere exchange

2.1. The atmospheric boundary layer

The atmospheric boundary layer is defined as the lower part of the atmosphere that is in direct contact with the Earth's surface. The height of the atmospheric boundary layer reaches up to 100–3000 m above the ground surface, and varies diurnally and seasonally (Wild and Jones, 1995; Harner et al., 1995; Cousins et al., 1999c; Lee et al., 1998; Farrar et al., 2005; Scholtz and Bidleman, 2006, 2007; MacLeod et al., 2007; Tao et al., 2007). Transport of airborne pollutants in the atmospheric boundary layer mainly depends on eddy diffusion, which in turn is related to wind velocity and surface roughness. Wind velocity is dependent on many factors and conditions at varying scales, e.g. on pressure gradients and on local weather conditions. Under neutral or stable atmospheric conditions, i.e. when vertical air movement does not take place beyond the rate of adiabatic heating or cooling, wind velocity and direction primarily varies horizontally. The horizontally moving air carries momentum, water vapor, heat, and chemicals, which results in turbulent transport of these components also perpendicular to the mean wind direction.

2.2. Time-dependent accumulation of SVOCs in soils

The history of SVOCs accumulation in soils, especially for PCBs and organochlorine pesticides, can be traced through a simple conceptual model (depicted in Fig. 1) that includes two phases: a pollution period and a regulation period. Prior to industrialization, natural emissions had already resulted in a low background pollution of soils with SVOCs, but with the onset of industrial revolution in the 19th century, anthropogenic activities significantly increased the amount in the environment. Generally, the highest concentrations of SVOCs in the environment were observed in the 1960s and 1970s. In the late decades of the 20th century, regulatory policies for responsible energy consumption and economic development as well as international source reduction measures have been enacted to protect the environment. Since then a continuous decrease in concentrations of many environmental pollutants has been observed in industrialized countries (Gocht and Grathwohl, 2004; Prevedouros et al., 2004; Schuster et al., 2010). As a consequence, the concentrations of SVOCs in soils (black solid lines in Fig. 1) are expected to decrease when compared to the hypothetical case in which no reduction measures were applied (gray dashed line in

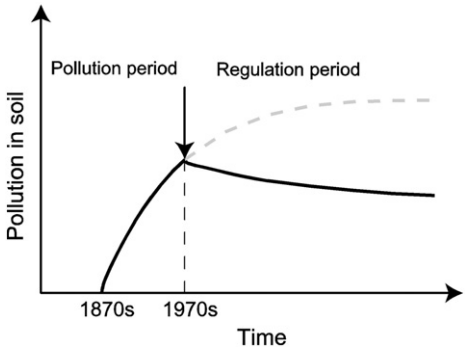

Fig. 1. Simplified temporal trend for the accumulation of SVOCs in soils during the high pollution period (from ca. 1870 to 1970) and the subsequent regulation period (since ca. 1970). Eventually, steady-state conditions will establish because of biodegradation and leaching towards groundwater; the gray dashed line refers to the case in which no environmental reduction measures have been applied, whereas the black solid line accounts to a 50% decrease of pollutant input (after the 1970s), e.g. because of environmental regulations (from numerical simulation).

Fig. 1). SVOCs present in the soil eventually may undergo degradation by microorganisms, re-volatilize to the atmosphere because of reduced atmospheric concentrations, and/or leach to the underlying groundwater. In early-industrialized countries such as Germany, over the last two centuries a similar trend with respect to the accumulation of PAHs in soils or sediments was observed (Gocht and Grathwohl, 2004). In fact, due to technological progress and regulation nowadays significantly less PAHs are emitted into the atmosphere than in the middle of the last century.

3. Numerical simulations and parameters

3.1. Physico-chemical parameters of phenanthrene

Phenanthrene was chosen as a representative model compound, because it has physico-chemical properties (hydrophobic, lipophilic) similar to many other SVOCs. Furthermore, phenanthrene is widely spread in the atmosphere and, thus, significantly contributes to the high concentrations of this pollutant in topsoils, e.g. in Germany (Gocht et al., 2001, 2007). As phenanthrene is a relatively easily degradable compound under aerobic conditions, the role of biodegradation on the long-term fate of this compound in soils can be studied.

Several studies on the environmental fate and the transport of phenanthrene in soils provide reliable data on sorption and biodegradation processes. Phenanthrene is mainly present as vapor in the free atmosphere or sorbed to the soil organic carbon. Sorption/desorption equilibrium of phenanthrene in fine grained soils or sediments (particle size less than 0.1 mm) was shown to occur in typical time scales of few weeks, and certainly in less than one year (Rügner et al., 1999; Kleineidam et al., 1999, 2002, 2004; Karapanagioti et al., 2000; Wang et al., 2007; Kuntz and Grathwohl, 2009). Therefore, for the time periods relevant in this study (years to centuries) sorption/desorption at the grain scale can be considered as a local equilibrium process. Table 1 summarizes the relevant physico-chemical properties of phenanthrene used in the numerical simulations.

3.2. Conceptual model

A vertical 1-D model was applied to describe soil–atmosphere exchange of SVOCs (Fig. 2). We considered an open two-compartment model, in which a 100 m thick atmospheric boundary layer overlies a soil compartment with two soil layers, namely a 0.1 m thick topsoil layer with elevated organic carbon content and the vadose zone (subsoil layer) above a groundwater table at 5 m depth.

The two soil layers primarily consist of sandy material and are distinct from each other by different porosity, organic carbon content, and water saturation (Table 2). An average value of the organic carbon content of 3% (mean f_{OC}-case) was chosen for the topsoil layer, which approximates the average for European countries (Panagos et al., 2013). The organic carbon content in the subsoil was assumed to be ten times smaller than that in the topsoil. Low and high f_{OC}–cases (1% to 10%) were simulated since data on the spatial distribution of organic carbon content in soils, collected by the European Soil Data Centre, indicate a high natural variability of organic carbon contents ranging from 0.01% to over 35%. Potential co-transport of phenanthrene with dissolved organic carbon (DOC) in the soil water would be less significant than the effect of variability in soil organic carbon content and therefore was not considered (with DOC concentrations of less than 20 mg/L, the expected change in sorption of phenanthrene would be less than 20%). Potential changes in the organic carbon content of soils were accounted for by comparing the three different levels of f_{OC}.

A vertical water saturation profile was implemented using the well-known van Genuchten parameterization (e.g., Carsel and Parrish, 1988). The values of the van Genuchten parameters used in this study are given in Table 2.

The soil compartment was implemented as a 3-phase system with solid, aqueous, and gaseous phases. Phenanthrene is transported in the gaseous and aqueous phases, and partitions among the three different phases. In the atmosphere gaseous and aqueous phase transport was considered, whereas particle-associated deposition of airborne phenanthrene was not investigated in our study.

By implementing a first-order chemical reaction in the aqueous phase, we accounted for microbial degradation of phenanthrene in the subsurface:

$$C_{14}H_{10}(aq) + 16.5O_2 + 9H_2O \rightarrow 14CO_3^{2-} + 28H^+.$$

The reaction rate for microbial degradation of aqueous phenanthrene, with a half-life ($t_{1/2,biodeg} = \ln(2)/\lambda$ [s]), was assumed to be temperature independent.

In addition, bioturbation in soils (i.e., by feeding and burrowing of earthworms or other animals) (Cousins et al., 1999c) or plowing activities on agricultural land may have a strong effect on vertical mixing, and thus on mass transport. Bioturbation is very species specific and hence hard to quantify (Hedman, 2008). In this study, therefore,

Table 1
Physico-chemical properties of phenanthrene at 25 °C.

Chemical name	Unit	Value	Reference
Molecular weight, *MW*	g/mol	178.2	Schwarzenbach et al. (2003)
Overall half-life of biodegradation, $t_{1/2,biodeg}$	Hours	1.60×10^3	Gouin et al. (2000)
Aqueous diffusion coefficient, D_w^*	m^2/s	6.71×10^{-10}	Grathwohl (1998)
Gaseous diffusion coefficient, D_g^*	m^2/s	5.97×10^{-6}	Grathwohl (1998)
Water solubility, *S*	g/m^3	1.1	Schwarzenbach et al. (2003)
Subcooled liquid solubility, S_{sub}	g/m^3	3.05	Liu et al., (2013b)
Henry's law coefficient, *H*	Dimensionless	1.0×10^{-3}	Verschueren (1983)
Enthalpy of air–water partitioning, ΔH_{aw}	kJ/mol	47	Schwarzenbach et al. (2003)
Enthalpy of sorption, $\Delta H_{sorption}$	kJ/mol	−30	Wang and Grathwohl (2013)

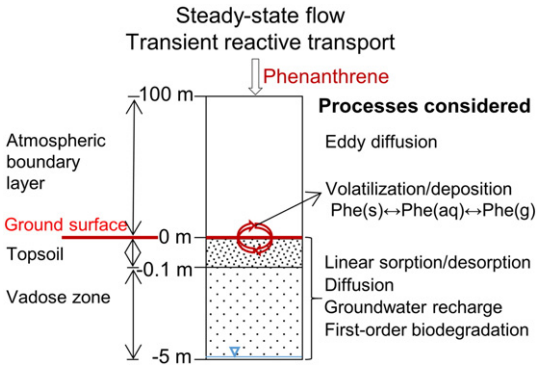

Fig. 2. Conceptual model of soil–atmosphere exchange of phenanthrene ('Phe') with a 100 m thick atmospheric boundary layer (not drawn to scale), a 0.1 m thick topsoil layer, and a 4.9 m thick vadose zone above the groundwater table.

we focus on undisturbed soils, i.e. without additional mixing due to bioturbation and plowing. Modeling was limited to steady-state flow of water and temperature was assumed to stay constant. In an earlier study, Kuntz and Grathwohl (2009) showed that the assumption of steady-state flow is justified to be representative for the prediction of long-term average concentrations of compounds in seepage water (i.e. average concentrations obtained from transient simulations are very close to concentrations from steady-state simulations in most cases of mid latitude precipitation frequency and intensity). At the upper boundary of the domain (Fig. 2), water infiltrates at a fixed rate and is allowed to discharge freely via the bottom boundary (i.e. free seepage boundary at $Z = -5$ m). A groundwater recharge rate of 200 mm/year and an average annual temperature of 10 °C were assumed, representative for the weather conditions in Germany (data from the German Weather Service, DWD, and the Federal Institute for Geosciences and Natural Resources, BGR).

3.3. Model description

The numerical code MIN3P was used to simulate soil–atmosphere exchange of phenanthrene and its reactive transport towards the groundwater table. MIN3P couples Richards' equation, the governing equation for water flow under variably saturated conditions, with reactive advective–dispersive transport in the aqueous phase and diffusive transport in the gaseous phase (Mayer et al., 2002). A generalized formulation for multicomponent, kinetically controlled and equilibrium biogeochemical reactions is integrated in the model.

Table 2
Physical and hydraulic parameters used in our conceptual model for the two soil layers.

Input parameter	Unit	Subsoil layer	Topsoil layer
Porosity, n	Dimensionless	0.33	0.40
Organic carbon content, f_{OC} (low f_{OC}-case)	Dimensionless	0.1%	1%
Organic carbon content, f_{OC} (mean f_{OC}-case)	Dimensionless	0.3%	3%
Organic carbon content, f_{OC} (high f_{OC}-case)	Dimensionless	1%	10%
Residual water saturation, S_{rw}	Dimensionless	0.2	
van Genuchten parameter, α	1/m	14.5	
van Genuchten parameter, N	Dimensionless	2.68	
van Genuchten parameter, l	Dimensionless	0.5	
Hydraulic conductivity, K	m/s	8.3×10^{-5}	
Dispersivity, α^*	m	0.01	
Groundwater recharge rate, q	mm/year	200	
Solids density, ρ	kg/m^3	2650	

3.3.1. Governing equations for flow

The governing differential equation for the simulation of variably saturated water flow is:

$$S_w S_s \frac{\partial h_\psi}{\partial t} + n\frac{\partial S_w}{\partial t} - \frac{\partial}{\partial z}\left[k_{rw} K \frac{\partial}{\partial z} h_\psi\right] = 0 \quad (1)$$

where S_w [−] and S_s [1/m] refer to the water saturation and the specific storage coefficient, and k_{rw} [−] and K [m/s] identify the relative permeability and the hydraulic conductivity, respectively. h_ψ [m] is the hydraulic potential, n [−] denotes the porosity, and t [s] is the time. In Eq. (1), we used the van Genuchten model to parameterize the vertical distributions of water saturation and relative permeability:

$$S_w = S_{rw} + \frac{1 - S_{rw}}{\left(1 + |\alpha\psi_a|^N\right)^m} \quad (2)$$

$$k_{rw} = S_{ew}^l \left[1 - \left(1 - S_{ew}^{1/m}\right)^m\right]^2 \quad (3)$$

with

$$m = 1 - 1/N \quad (4)$$

$$S_{ew} = \frac{S_w - S_{rw}}{1 - S_{rw}} \quad (5)$$

where S_{ew} [−] and S_{rw} [−] are the effective and the residual water saturation, ψ_a [m] denotes the matric potential, and l [−], α [1/m], m [−] and N [−] are the van Genuchten parameters (e.g., Carsel and Parrish, 1988). The same equations outlined above were also applied in the atmospheric boundary layer, where we assumed a uniform distribution of the aqueous phase with a very low water saturation of 3×10^{-5} (Fig. 3). Flow was at steady state and fixed to a rate of 200 mm/year.

3.3.2. Reactive transport modeling

The reactive transport process includes advective–dispersive transport of dissolved species, vapor phase diffusion, and the contributions from biogeochemical reactions that involve gaseous, aqueous, and mineral species in soil and the atmosphere:

$$\frac{\partial}{\partial t}[n_w c_w] + \frac{\partial}{\partial t}[n_g c_g] + \frac{\partial}{\partial z}[q c_w] - \frac{\partial}{\partial z}\left[D_{ew}\frac{\partial}{\partial z} c_w\right] - \frac{\partial}{\partial z}\left[D_{eg}\frac{\partial}{\partial z} c_g\right] - Q = 0 \quad (6)$$

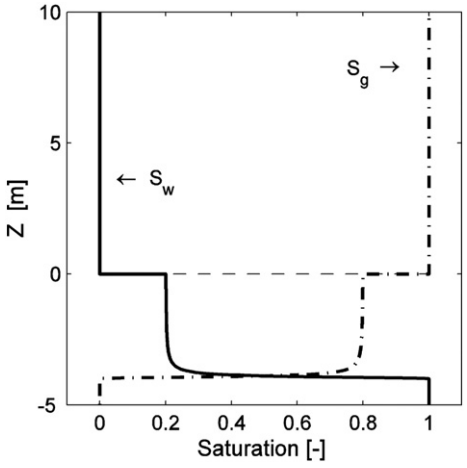

Fig. 3. Vertical profiles of water saturation (S_w) and gas saturation ($S_g = 1 - S_w$) across the soil–atmosphere interface (horizontal dashed line at $Z = 0$ m).

where c_w [kg/m^3] and c_g [kg/m^3] respectively are the concentrations of the compound of interest in the aqueous and gaseous phase; n_w [−] and n_g [−] denote the water-filled and gas-filled porosity, q [m/s] is the groundwater recharge rate, and Q [kg/(m^3·s)] represents the sink terms that result from biogeochemical reactions. In the present case, the parameter Q accounts for

$$Q = \lambda n_w c_w \tag{7}$$

where λ [1/s] refers to the biogeochemical reaction rate constant.

In Eq. (6), D_{eg} [m^2/s] and D_{ew} [m^2/s] are the effective diffusion coefficients in the gaseous and aqueous phases. The effective diffusion coefficient in the gaseous phase, D_{eg} [m^2/s], is estimated according to the empirical correlation from Moldrup et al. (2000):

$$D_{eg} = D_g^* \frac{n_g^{2.5}}{n} \tag{8}$$

where D_g^* [m^2/s] is the molecular diffusion coefficient of the diffusing compound in the free gaseous phase.

To compute the effective diffusion/dispersion coefficient in the aqueous phase, D_{ew} [m^2/s], we extended Eq. (8) (Moldrup et al., 2000, 2001):

$$D_{ew} = \alpha^* |q| + D_w^* \frac{n_w^{2.5}}{n} \tag{9}$$

where α^* [m] is the dispersivity of the porous medium and D_w^* [m^2/s] denotes the molecular diffusion coefficient of the transported compound in the free aqueous phase. The values of D_g^* (Eq. (8)) and D_w^* for phenanthrene at 25 °C are listed in Table 1.

At the soil–atmosphere interface, hence, the dominating transport mechanism shifts from pure diffusion in the soil to eddy diffusion in the atmosphere. Typically, the eddy diffusion coefficient, D_{eddy} [m^2/s], is used to describe turbulent mixing in the atmospheric boundary layer. Under neutral or stable atmospheric conditions, D_{eddy} was shown to linearly increase with height (Foken, 2008):

$$D_{eddy} = k u_* Z \tag{10}$$

where k [−] represents the von Kármán constant (here $k = 0.4$), u_* [m/s] is the friction or shear velocity (here 0.3 m/s), and Z [m] refers to the height above the ground surface (with $Z = 0$ m at the surface). To account for the turbulent mixing in MIN3P, D_{eg} in Eq. (6) was replaced by D_{eddy} (Eq. (10)) in the atmospheric boundary layer. Fig. 4 shows

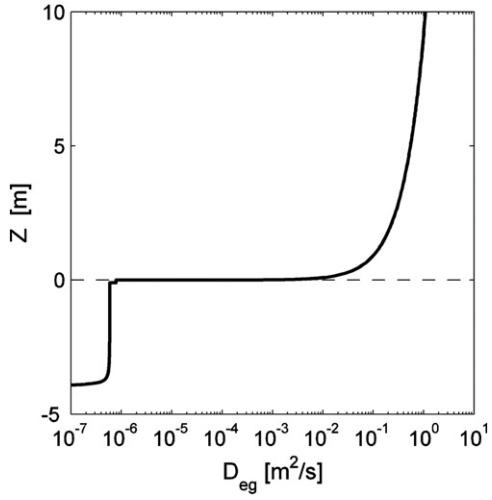

Fig. 4. Vertical profile of the effective diffusion coefficient of gaseous phenanthrene across the soil–atmosphere interface (horizontal dashed line at $Z = 0$ m) at 10 °C at a bare soil site. The x-axis is shown in log-scale.

the effective diffusion coefficients used in the model at 10 °C and at a bare soil site (comparable values for eddy diffusion in the atmosphere depicted by Meixner et al., 2003). The linear model for eddy diffusion is based on the assumption that atmospheric conditions are neutral or stable, i.e. vertical air movement does not take place beyond the rate of adiabatic heating or cooling. Non-linear parameterizations would cause more mixing due to increased eddy diffusion.

3.3.3. Distribution in the 3-phase system

We assumed that phenanthrene distributes linearly among the solid, the aqueous, and the gaseous phases. Partitioning of phenanthrene between the aqueous and the gaseous phases is described by Henry's law:

$$c_g = H c_w \tag{11}$$

in which H [−] is the temperature-dependent Henry's law coefficient.

Distribution of phenanthrene between the aqueous and the solid phases is described by:

$$c_s = K_d c_w \tag{12}$$

where c_s [kg/kg bulk phase] denotes the solid phase concentration and K_d [L/kg] is the distribution coefficient calculated for organic compounds by:

$$K_d = K_{OC} f_{OC} \tag{13}$$

where f_{OC} [−] is the soil organic carbon content and K_{OC} [L/kg] is the soil organic carbon–water partition coefficient. The latter was calculated by a linear regression, reported in Razzaque and Grathwohl (2008), which is based on the subcooled liquid solubility, S_{sub} [kg/L], of the compound of interest:

$$\log K_{OC} = -0.85 \log S_{sub} - 0.55 \tag{14}$$

with an average absolute error of 0.23 log units in predicted K_{OC} values.

3.3.4. Temperature dependence of parameters

In Table 1 the physico-chemical parameters for phenanthrene were given for 25 °C. To account for low subsurface temperatures of 10 °C, the molecular diffusion, sorption and Henry's law coefficients were converted by applying empirical relationships. Temperature dependence of the molecular gas diffusion coefficient according to Lyman et al. (1990) is:

$$\frac{D_g(T)}{D_g(T_0)} = \left(\frac{T}{T_0}\right)^{1.75} \tag{15}$$

where T [K] is the specified temperature and T_0 [K] refers to the standard temperature (298.15 K).

The temperature dependence of the molecular diffusion coefficient in water was computed according to Atkins (1986):

$$\frac{D_w(T)}{D_w(T_0)} = \frac{T}{T_0} \times 10^{\frac{247.8(T-T_0)}{(T-140)(T_0-140)}}. \tag{16}$$

In addition, to account for the temperature dependence of the sorption distribution coefficient, K_d [L/kg], we applied the van't Hoff equation:

$$\frac{K_d(T)}{K_d(T_0)} = \exp\left[-\frac{\Delta H_{sorption}}{R}\left(\frac{1}{T} - \frac{1}{T_0}\right)\right] \tag{17}$$

where $\Delta H_{sorption}$ [kJ/mol] is the enthalpy of sorption with a representative value of −30 kJ/mol for phenanthrene for anthropogenic and mineral soil samples (see Wang and Grathwohl, 2013). R [J/(mol K)] refers to the ideal gas constant with a value of 8.314 J/(mol K).

To calculate the temperature dependence of Henry's law coefficient, the van't Hoff equation (Eq. (18)) was used again, accounting for the enthalpy of air–water partitioning, ΔH_{aw} [kJ/mol], of 47 kJ/mol for phenanthrene (see Schwarzenbach et al., 2003).

3.4. Model simulations performed

As the base scenario, we started from clean soil (initial condition $c_w(Z, t_0) = 0$) and allowed pollution of the soil during a 100 years pollution period (Fig. 1). This assumption seems justified since preindustrial emission rates were at least ten times smaller than during industrialization as shown by the sedimentary record in lakes and estuaries (Müller et al., 1977; Sanders et al., 1993; Simcik et al., 1996; Schneider et al., 2001; Lima et al., 2003). The vertical concentration profile, observed at the end of the pollution period then was taken as the initial condition for the subsequent regulation period, where we assumed 50% reduced concentrations of pollutants in the atmosphere. This is a reasonable assumption for early-industrialized countries such as Germany. In newly industrialized countries such as China as well as developing countries atmospheric concentrations may still increase (Liu et al., 2013a).

The atmospheric concentrations of phenanthrene during the pollution and regulation periods were predefined in the model (boundary conditions). We calculated the average gaseous concentration of phenanthrene in the atmosphere, with a value of 2.24 ng/m^3, from data of 85 passive sampler stations in 32 European countries in 2006 (EMEP database) (regulation period). Before environmental regulations came into effect (pollution period), the gaseous concentration of phenanthrene was assumed to be twice as high (Gocht and Grathwohl, 2004).

3.4.1. Model verification and scenarios

Verifications of the numerical model with analytical solutions are shown in Appendix A. Excellent agreement of the numerical results with analytical solutions proved the applicability of our numerical model to simulate soil–atmosphere exchange. We used the extended version of the numerical code to investigate the long-term environmental fate of SVOCs between soils and the atmosphere. Model runs were performed in order:

(i) to investigate the importance of the atmospheric boundary layer for the uptake of airborne phenanthrene in soil (Table 2) during the early pollution period.
(ii) to quantify the relative importance of sorption, groundwater recharge, biodegradation, and diffusion on the uptake of airborne phenanthrene in soil. To do so, we performed a local sensitivity analysis on the relevant parameters by comparing vertical concentration profiles for the mean f_{OC}–case as well as the change in total mass of phenanthrene present in the soil compartment for the high and low f_{OC}–cases (Table 2).
(iii) to evaluate the change in vertical concentration profiles of phenanthrene in the soil due to reduced anthropogenic emissions and, hence, temporary re-volatilization from the soil to the atmosphere, following the 100 years pollution period. Our model results are qualitatively compared to field observations from several studies in Europe.
(iv) to estimate the time scales needed to reach steady state for three different levels of f_{OC}.

Vertical concentration profiles are shown as relative gaseous concentration, c/c_0 [−], in which c_0 is the atmospheric concentration of phenanthrene (4.48 ng/m^3) applied as a boundary condition at the upper limit of the model domain during the pollution period. The time-dependent accumulation of phenanthrene in the soil compartment is shown as the relative mass, $M/M_{100\ year}$ [−], in which $M_{100\ year}$ [kg] is the total mass of phenanthrene, present in the soil, at the end of the 100 years pollution period.

4. Results and discussion

4.1. Effect of the atmospheric boundary layer

To evaluate the importance of the atmospheric boundary layer for uptake and re-volatilization of SVOCs in soils, we placed the upper boundary condition directly at the ground surface ($Z = 0$ m) and compared the results to the outcomes of a second simulation with a 100 m thick atmospheric boundary layer ($Z = 100$ m). Fig. 5 shows the vertical concentration profiles of gaseous phenanthrene for the two simulations at 1 day, 30 days, and 1000 days.

Due to fast eddy diffusion, the atmospheric boundary layer is well mixed as shown by the straight vertical concentration profiles (red dashed lines) in Fig. 5. Only at early times (1 day and 30 days, Fig. 5A and B), mixing near the soil–atmosphere interface is not complete, which thus affects the concentration distribution in the soil compartment underneath. In fact, by comparing the two simulation results with each other in Fig. 5A and B, for short time periods we observe a slight lag in mass transport of phenanthrene in the soil in case the atmospheric boundary layer is included. However, for 1000 days (Fig. 5C), the lag between the two simulations has disappeared. The shape of the breakthrough curves in the soil indicates that at early times (i.e. within the first month) transport of phenanthrene is dominated by vapor phase diffusion in the soil. Generally, our results show that at time scales larger than one month the atmospheric boundary layer has a negligible effect on mass transport of atmospheric pollutants into soils — provided that pollutants are constantly supplied to the atmosphere. In the following, we therefore neglect the atmospheric boundary layer. It should be noted, however, that for highly volatile less sorbing compounds ("gases") and for indoor situations the atmospheric boundary layer may be important for mass transfer.

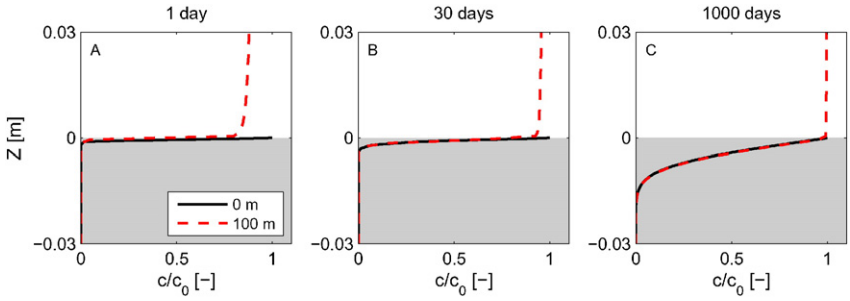

Fig. 5. Impact of the atmospheric boundary layer on uptake of vapor phase phenanthrene into the soil (mean f_{OC}–case, Table 2); black solid lines: concentration profiles in the absence of the atmospheric boundary layer, i.e. upper boundary condition at $Z = 0$ m; red dashed lines: concentration profiles in the presence of the atmospheric boundary layer, i.e. upper boundary condition at $Z = 100$ m. The gray-shaded areas indicate the location of the topsoil layer enriched in organic carbon.

4.2. Sensitivity analysis on the relevant transport parameters

To determine which physico-chemical parameters are decisive for soil–atmosphere exchange of atmospheric pollutants, we performed a local sensitivity analysis by subsequently changing one of the following parameters: the sorption distribution coefficient (sorption, + 50%), the groundwater recharge rate (advection, + 50%), the first-order biodegradation rate (biodegradation, + 50%), and the diffusion coefficients in the gaseous and aqueous phases (diffusion, + 50%). Such changes may be due to temperature fluctuations by 5 to 10 °C or uncertainty in parameter estimations. We investigated the impact of these parameters on the long-term vertical concentration profiles of phenanthrene in the soil at 1 year, 10 years, and 100 years during the pollution period.

Fig. 6 shows the concentration profiles in the soil (solid lines) as well as the results of our sensitivity analysis (dashed lines). With increasing organic carbon content in the soil, i.e. with increasing sorption to the solid phase, retardation increases and phenanthrene propagates more slowly into the soil (Group S in Fig. 6). In contrast, increasing the groundwater recharge rate (Group A in Fig. 6) results in more rapid downward advective transport of phenanthrene, whereas biodegradation hardly affects transport of phenanthrene at this time scale (Group B in Fig. 6; concentration profiles overlap each other almost entirely). In accordance with the findings of McKelvie et al. (2013), these results demonstrate how strong sorption and unsaturated conditions limit the effect of biodegradation on the propagation of phenanthrene in the soil, due to reduced bioavailability of the pollutant. Also, an increase in diffusion coefficients impacts the propagation of phenanthrene in the soil (Group D in Fig. 6). The shape of the breakthrough curves in Group D indicates that vapor phase diffusion and sorption dominate the transport process during the pollution period for the mean f_{OC}-case. Since diffusion and sorption are temperature sensitive and effective groundwater recharge is highly dependent on the local climate, diurnal and seasonal changes in temperature and groundwater recharge will introduce some dynamics in uptake and re-volatilization of SVOCs in/from soils. Model simulations considering diurnal changes of temperature and atmospheric boundary layer thickness are subject of ongoing work.

To quantify the impact of the different parameters on the total mass of phenanthrene accumulated in the soil, we also calculated the local sensitivity, which is defined as the relative deviation of the output value due to a change in an input value (Webster et al., 1998; Meyer et al., 2005). Local sensitivity, $S(X_i)$ [−], therefore, was computed as the relative deviation of the total mass, $\partial M(t) / M(t)$ [−], in the soil due to a 50% increase in the respective parameter, X_i (i.e. sorption distribution coefficient, groundwater recharge rate, biodegradation rate, and gaseous and aqueous diffusion coefficients):

$$S(X_i) = \left| \frac{\partial M(t) / M(t)}{\partial X_i / X_i} \right| \tag{18}$$

where $M(t)$ [kg] refers to the total mass of phenanthrene present in the soil at a selected time point, t [s]. In case $S(X_i) \le 0.1$, the total mass present in the soil is assumed to be non-sensitive to the input variable.

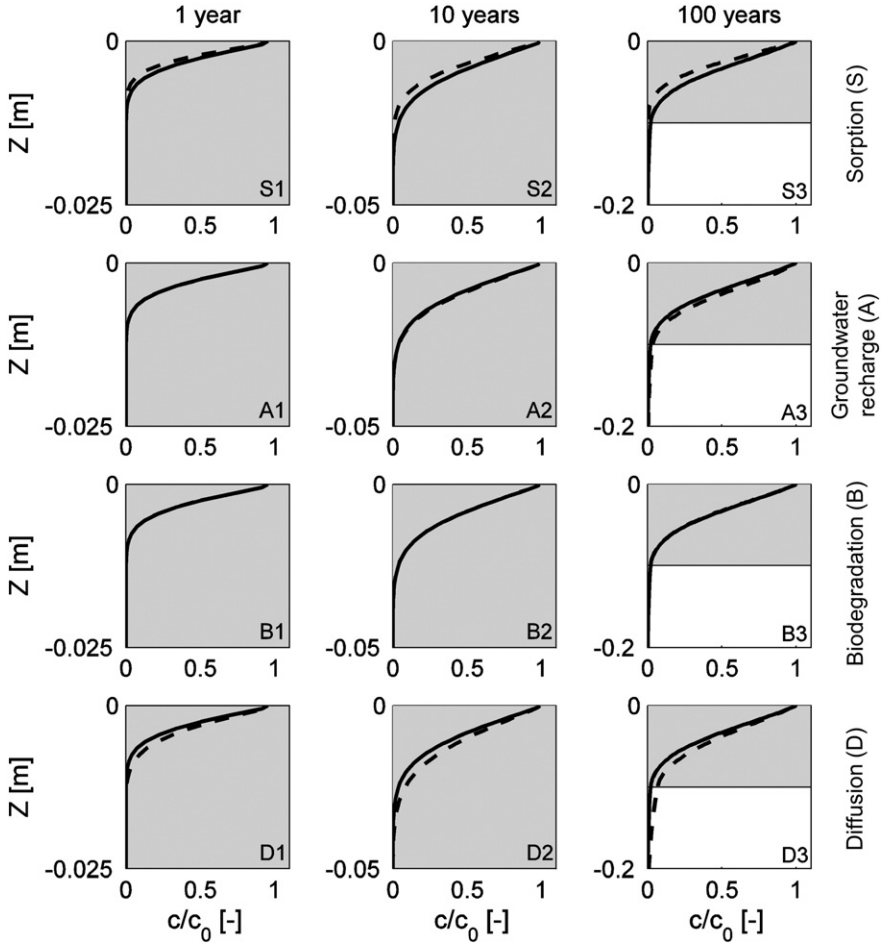

Fig. 6. Concentration profiles of phenanthrene in the soil at three time points during the uptake (pollution) period. The solid lines refer to concentration profiles for the mean f_{OC}-case, whereas the dashed lines refer to those with 50% increase in the respective parameter(s) investigated. Note different scales on the vertical axis. The gray-shaded areas indicate the location of the topsoil layer enriched in organic carbon.

With increasing local sensitivity, the total mass accumulated is increasingly affected by the input variable.

Fig. 7 shows the time-dependent local sensitivity of each parameter based on the total mass of phenanthrene accumulated in the soil for 7 time points (0.3 year, 1 year, 3 years, 10 years, 30 years, 50 years, and 100 years) and for the three levels of f_{OC}. We found that sorption (Fig. 7A) significantly affects mass accumulation at all times. In addition, diffusion (Fig. 7D) clearly dominates only at early times (up to 10 years), whereas it diminishes at later times and groundwater recharge (Fig. 7B) becomes more important. For the mean and the high f_{oc}-cases, accumulation is still not advection-dominated at the end of the pollution period (at 100 years); while for the low f_{oc}-case, advection already dominates the transport at 100 years. In fact, the higher the organic carbon content in the soil, the more delayed in time is the observed pattern in local sensitivity due to increased retardation from stronger sorption properties. As illustrated in Fig. 7C, the effect of biodegradation on mass accumulation is strongly constrained over the 100 years pollution period for the three levels of f_{oc} since steady state is not achieved yet. However, on even longer time scales biodegradation would take over and determine long-term mass accumulation (the stronger the sorption the longer that takes).

As to be expected, the total mass of phenanthrene in the soil is highly dependent on sorption at all times. Groundwater recharge and biodegradation determine the total mass present in the soil in the long term, while diffusion dominates the transport process at early times. Note, that for less sorbing compounds time scales would be much shorter.

4.3. Impact of reduced emissions: re-volatilization from soils

In the following, we investigate how a regulation period with a 50% reduction in anthropogenic emissions of phenanthrene after 100 years of pollution influences the concentration distribution across the soil–atmosphere interface. Fig. 8 shows the vertical concentration profiles across the soil–atmosphere interface at 1 year and 30 years after environmental protection measures became effective for the three levels of f_{OC} considered.

If the concentration in the atmosphere is reduced, re-volatilization of phenanthrene from the soil to the atmosphere occurs. In Fig. 8 this is indicated by a reversed concentration gradient that develops directly at the soil-atmosphere interface. Peak concentrations of phenanthrene are observed just below this interface. Over time, the peak shifts downwards and diminishes as phenanthrene re-volatilizes into the atmosphere and also migrates into deeper soil layers by diffusion and advection. The propagation of phenanthrene in the soil layers is affected by the organic carbon content of the soil. From the low f_{OC}-case, to the mean f_{OC}-case, to the high f_{OC}-case, advective transport of phenanthrene into the deeper soil layers is increasingly retarded while more phenanthrene diffuses back to the atmosphere if f_{OC} is high.

We qualitatively compared the results of our numerical simulations, shown in Fig. 8, to field observations of the vertical distribution of phenanthrene in soils, published in the late 1990s and early 2000s (Wilcke et al., 1996; Cousins et al., 1999b, 1999c; Krauss et al., 2000; Gocht et al., 2001; Vikesøe et al., 2002; Atanassova and Brümmer, 2004). In several field studies (Wilcke et al., 1996; Krauss et al., 2000; Gocht et al., 2001; Vikesøe et al., 2002; Atanassova and Brümmer, 2004) higher concentrations of phenanthrene in the topsoil than in the underlying subsoil were found, which generally matches results from our model scenario. Moreover, Cousins et al. (1999b) detected the highest concentration of total PAHs (with phenanthrene being the principal component in the upper soil layers according to Atanassova and Brümmer, 2004) at a depth of 5 cm below the ground surface. This finding is also in agreement with our model results at 30 years

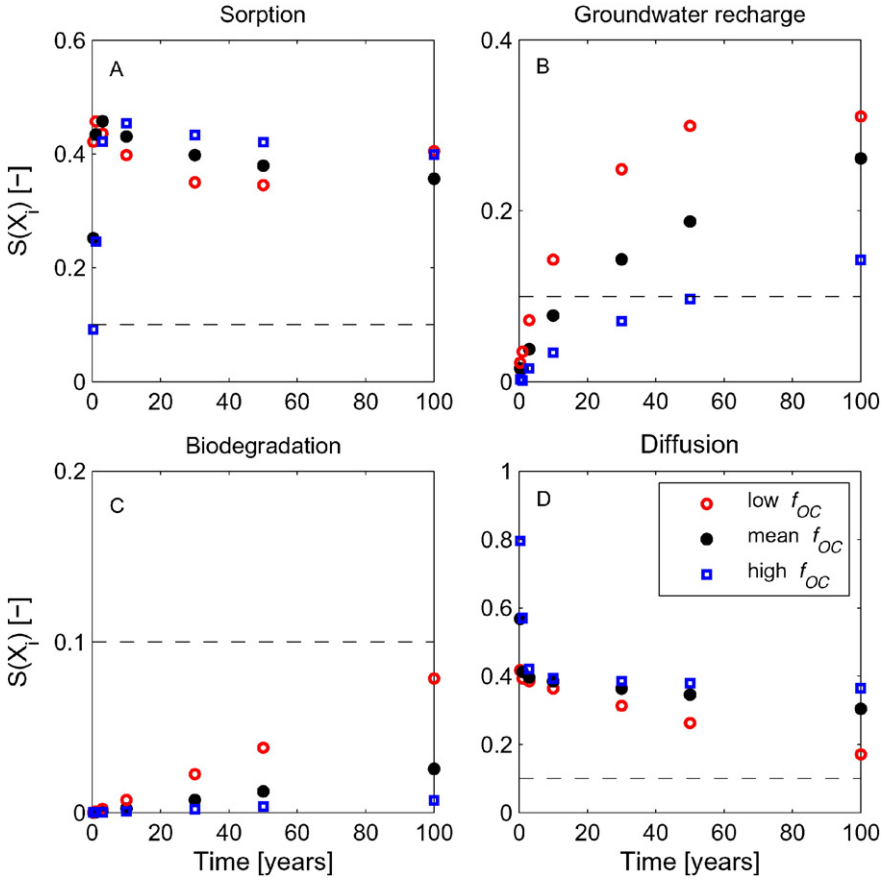

Fig. 7. Time-dependent local sensitivity ($S(X_i)$) of each parameter based on the total mass accumulated in the soil for the three levels of f_{OC}. The horizontal dashed line refers to a local sensitivity of 0.1 (below, the total mass in the soil is assumed to be non-sensitive to the input parameter). Note, different scales on the vertical axis.

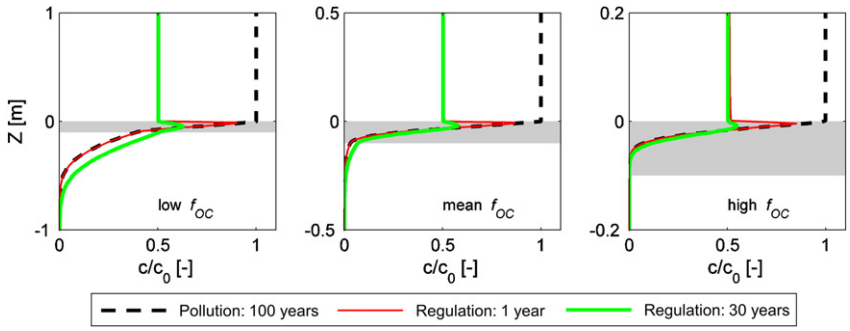

Fig. 8. Concentration profiles at the end of the pollution period (black dashed line), and 1 year and 30 years after environmental reduction measures became effective (solid lines) for the three levels of f_{oc}. On the vertical axis different scales are shown and the gray-shaded areas indicate the location of the topsoil layer. Only in the low organic carbon case the pollution penetrated the high organic topsoil.

after the start of the regulation period. In particular, Cousins et al. (1999b) reported values for temperature and organic carbon content that were similar to the values used for the mean f_{OC}-case in our study. The authors hypothesized that bioturbation is the main reason for the lower concentrations in the soil layer close to the ground surface. However, our model results indicate that re-volatilization and limited bioavailability because of strong sorption lead to a peak concentration at shallow depths below the ground surface.

4.4. Time scales for re-volatilization and for steady state in the soil

To estimate the time scale for re-volatilization from the soil, several model scenarios with and without environmental regulation measures or biodegradation were investigated. We extended our simulation period to 2500 years to account for long time scales involved.

Fig. 9 shows the accumulation of phenanthrene in the soil during the 100 years pollution period (black solid line) and the subsequent 900 years regulation period (black dot-dash line). As environmental reduction measures become effective, we observe a significant change in transport across the soil–atmosphere interface when compared to the non-regulated scenario (gray dashed line in Fig. 9). The reduced atmospheric concentration of phenanthrene during the regulation period results in a significantly lower amount of phenanthrene accumulating in the soil. With the onset of reduced anthropogenic emissions of phenanthrene to the atmosphere, we also observe re-volatilization of phenanthrene from the soil to the atmosphere that lasts for about 20 years (compare black dot-dash and dashed lines in Fig. 9) — after that the soil becomes a sink again.

Fig. 10 compares the accumulation of phenanthrene in the soil for the three levels of f_{OC}. In all three cases, retarded diffusion limits the transport of phenanthrene in the topsoil layer during the 100 years pollution period, resulting in the same mass accumulation of phenanthrene accumulating in the soil (linear partitioning). After the concentration of phenanthrene in the atmosphere is reduced by half, re-volatilization of phenanthrene from the soil to the atmosphere occurs and for a limited time period the soil becomes a secondary source for pollution. In the long term, however, the soil becomes a sink again and mass transport is determined by biodegradation and groundwater recharge. As expected, with increasing organic carbon content more phenanthrene accumulates in the soil (due to increased sorption). Also, the time needed to eventually reach steady state extends with increasing f_{oc}. We define the characteristic time for steady state, t_c [s], by the time period needed to reach 63.21% of the total mass in the soil at steady state (see details in the Appendix B where the governing equation was derived for a box model). For the low f_{OC}-case, the mean f_{OC}-case, and the high f_{OC}-case, the characteristic times for steady state following the reduction in atmospheric concentration are 143 years,

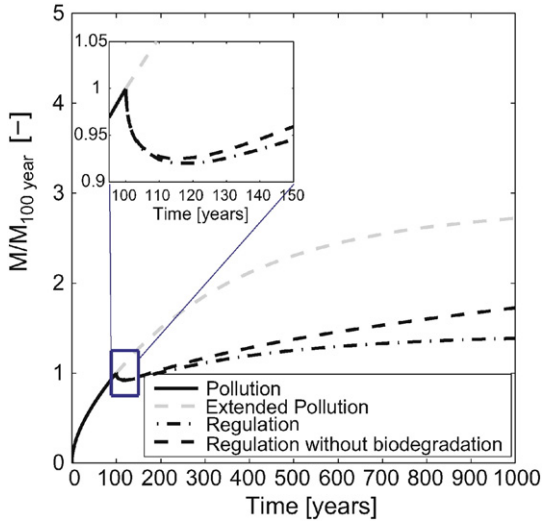

Fig. 9. Accumulation of phenanthrene in the soil (mean f_{OC}-case) for constant emission (solid black line or gray dashed line), and a reduction of emission rates by 50% after 100 years with and without biodegradation.

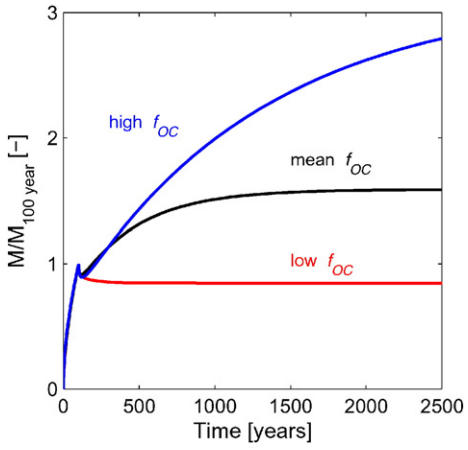

Fig. 10. Time-dependent mass accumulation of phenanthrene in the soil for the three levels of f_{OC}. Values of the sorption distribution coefficient K_d in the topsoils are 261.0 L/kg for the low-f_{OC} case (1%), 782.9 L/kg for the mean-f_{OC} case (3%), and 2609.8 L/kg for the high-f_{OC} case (10%), respectively.

430 years, and 1430 years, respectively (calculated by applying Eq. (B6) in the Appendix B, with a Damköhler number, *Da*, of 10).

5. Summary and conclusions

In this study, we extended the multicomponent reactive transport code MIN3P by an atmospheric boundary layer accounting for eddy diffusion. We used a vertical 1-D model (Fig. 1) to study soil–atmosphere exchange of SVOCs for non-disturbed soils with varying boundary conditions in the atmosphere (i.e. a decrease of pollutant concentration). Phenanthrene was used as a representative compound for SVOCs and was assumed to be supplied by continuous anthropogenic emissions to the atmosphere. Average values for temperature (10 °C) and groundwater recharge (200 mm/year) were applied in our model, and three cases with different organic carbon contents were analyzed for the specific base scenario in Germany.

We found that in the long term, the soil properties limited re-volatilization of phenanthrene into the atmosphere. Due to fast eddy diffusion and continuous anthropogenic emissions of gaseous phenanthrene, the atmospheric boundary layer is always mixed and thus has a negligible effect on the soil uptake of atmospheric pollutants, except for time periods < 1 month. This indicates that the atmospheric boundary layer is only relevant for short-term changes in the boundary conditions (emission rates, temperatures). Temperature-driven diurnal concentration changes and the height and the stability of the atmospheric boundary layer do not affect the long term uptake and release of pollutants from soils.

A sensitivity analysis showed that sorption/desorption was the most relevant process at all times, whereas vertical transport by diffusion was relevant only in the short term (years to decades) whereas groundwater recharge dominated transport in the long term (decades to centuries). Biodegradation was slowed down by sorption, and thus was of lower relevance.

Re-volatilization of SVOCs from soils to the atmosphere occurs only for a relatively short time period after environmental regulation measures came into effect (i.e. only over two decades for the specific exposure scenario investigated in this study with an abrupt drop in atmospheric concentrations). Gradually decreasing pollutant levels in the atmosphere would cause even less re-volatilization. Thus, soils are more or less infinite sinks for atmospheric pollutants even if concentrations are reduced by 50%. A simple analytical solution can be applied to estimate the time periods needed to reach steady state between input and biodegradation rates (see Appendix B) and the concentration levels in the soil at steady-state conditions. For phenanthrene (representative for many PAHs) steady-state time scales amount to centuries to millennia depending on soil organic carbon content and the thickness of the soil layer considered. The extended MIN3P code presented in this study can also be applied to simulate soil–atmosphere exchange of other atmospheric pollutants (e.g. further PAHs, PCBs, pesticides) or semi-volatile compounds (e.g. O_2, CO_2).

Acknowledgment

We acknowledge funding by the DFG (German Research Foundation) through the International Research Training Group 'Integrated Hydrosystem Modelling' (GRK 1829/1). The authors thank Prof. David W. Blowes at the University of Waterloo for helpful discussions and comments of this paper.

Appendix A. Results of model verification, using the extended MIN3P code and well-known analytical solutions

A.1. Transport by advection–dispersion and diffusion

To verify the numerical code, we modeled transport through a 5 m thick homogeneous soil column (porosity = 0.33; organic carbon content = 0.3%; temperature = 10 °C) and compared the results of our numerical simulations with corresponding analytical solutions for advective–dispersive transport (Ogata and Banks, 1961) and diffusion into a semi-infinite porous medium with linear sorption (Grathwohl, 1998).

The analytical solution for advective–dispersive transport (Ogata and Banks, 1961) in a water-saturated porous medium is:

$$\frac{c}{c_0} = \frac{1}{2}\left[erfc\left(\frac{|Z| - \frac{q}{n}t}{2\sqrt{Dt}}\right) + \exp\left(\frac{\frac{q}{n}|Z|}{D}\right) erfc\left(\frac{|Z| + \frac{q}{n}t}{2\sqrt{Dt}}\right)\right] \quad \text{(A1)}$$

where c/c_0 [−] is the normalized concentration of a conservative tracer, $|Z|$ [m] refers to the soil depth (i.e. $Z = 0$ at the ground surface), q [m/s] is the steady-state seepage water recharge rate (here 200 mm/year), n [−] denotes the total porosity, and t [s] is the time. D [m^2/s] denotes the hydrodynamic dispersion coefficient:

$$D = \frac{\alpha^*|q|}{n} + D_w^* n^{0.5} \quad \text{(A2)}$$

where α^* [m] refers to the dispersivity of the porous medium (here: $\alpha^* = 0.01$ m) and D_w^* [m^2/s] is the molecular diffusion coefficient of the compound of interest in water (phenanthrene: 6.71×10^{-10} m^2/s).

For pure diffusive transport we compared the numerical results with the analytical solution for retarded diffusion into a partially water-saturated semi-infinite porous medium (Grathwohl, 1998):

$$\frac{c}{c_0} = erfc\left(\frac{|Z|}{2\sqrt{D_a t}}\right) \quad \text{(A3)}$$

where D_a [m^2/s] denotes the apparent diffusion coefficient of a vapor phase compound in porous media:

$$D_a = \frac{D_{eg}}{n_g + \frac{n_w}{H} + \frac{\rho(1-n)K_d}{H}} = \frac{D_g^* \frac{n_g^{2.5}}{n}}{n_g + \frac{n_w}{H} + \frac{\rho(1-n)K_d}{H}} \quad \text{(A4)}$$

where D_{eg} [m^2/s] and D_g^* [m^2/s] are the effective and the molecular gas diffusion coefficients, n_g [−] and n_w [−] are the gas-filled and the water-filled porosity, and H [−], ρ [kg/m^3], K_d [L/kg], S_g [−], and S_w [−] denote the Henry's law coefficient, the density of the particles, the sorption distribution coefficient, the gas saturation, and the water saturation, respectively.

Our results for the two cases are shown in Fig. A1. For both cases we achieved excellent agreement between the numerical model results and the analytical solutions. Besides numerical accuracy, this confirms accurate implementation of transport parameters (recharge, dispersion and diffusion coefficients, sorption, air-water partitioning, etc.).

Appendix B. Characteristic time scales, steady-state concentrations and Damköhler numbers

For estimation of characteristic time scales to achieve steady state and corresponding concentration levels an analytical solution was derived using a simple box model. As described above, a uniform, water-saturated 5 m thick soil compartment was considered (porosity = 0.33; organic carbon content = 0.3%; temperature = 10 °C). Taking into account only groundwater recharge (which dominates over diffusion in the long term), linear sorption, and first-order biodegradation, the total solute mass change per area, $\frac{dM}{dt}$ [mg/(m^2·s)], in the soil results in the following differential equation:

$$\frac{dM}{dt} = \text{input} - \text{decay} - \text{output} = qc_{w,in} - \lambda c_w \theta h - qc_w \quad \text{(B1)}$$

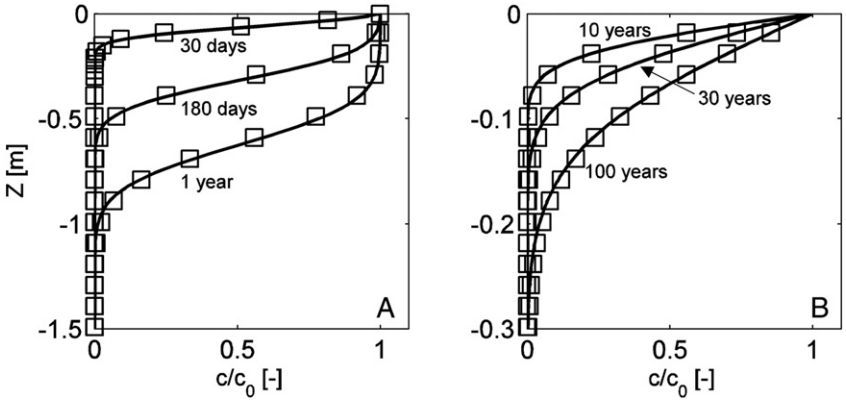

Fig. A1. Verification of MIN3P (symbols) with analytical solutions (lines) for fixed concentration at the top boundary: (A) conservative advective–dispersive transport under water-saturated conditions, (B) retarded diffusion in the unsaturated soil ($K_d = 78.3$ L/kg).

h [m] is the thickness of the soil layer considered and q [m/s] denotes the infiltration rate, which at steady state is equal to the groundwater recharge rate. $c_{w,in}$ [kg/m^3] and c_w [kg/m^3] refer to the aqueous concentration at the inflow boundary and the aqueous concentration leaving the system. θ [−] represents the volumetric water content in the porous medium, and λ [1/s] is the rate constant of first-order biodegradation.

The total mass in a soil column, e.g. after breakthrough at depth h, is given by:

$$M = c_w\theta h + c_g(n-\theta)h + c_s\rho(1-n)h = c_w h(\theta + (n-\theta)H + \rho(1-n)K_d) \quad \text{(B2)}$$

where c_g [kg/m^3], and c_s [kg/kg bulk phase] respectively are the concentrations in the gas, and solid phase, and ρ [kg/m^3] denotes the solids density (2650 kg/m^3).

Since phenanthrene preferentially is present in the solid phase, M in Eq. (B2) can be simplified by neglecting the terms representing the gas and water phases ($M = h\rho(1-n)K_d c_w$). Integration of Eq. (B1) with respect to c_w and t yields:

$$\int_0^{c_w} \frac{dc_w}{(q+\lambda h\theta)c_w - qc_{w,in}} = -\int_0^t \frac{dt}{h\rho(1-n)K_d}. \quad \text{(B3)}$$

Thus,

$$\frac{c_w}{c_{w,in}} = \frac{1}{1+\lambda h\theta/q}\left(1-\exp\left(-\frac{q+\lambda h\theta}{h\rho(1-n)K_d}t\right)\right). \quad \text{(B4)}$$

In Eqs. (B3) and (B4), c_w is the averaged concentration in the aqueous phase across the soil depth. At $t = 0$, $c_w = 0$. Similarly, when $t \to \infty$ the steady-state concentration, $c_{w,s-s}$ [kg/m^3], is reached:

$$c_{w,s-s} = \frac{1}{1+\lambda h\theta/q}c_{w,in}. \quad \text{(B5)}$$

A characteristic time, t_c [s], to reach steady state may be defined for an argument of one in the exponential function of Eq. (B4):

$$t_c = \frac{h\rho(1-n)K_d}{q+\lambda h\theta}. \quad \text{(B6)}$$

Since $1-\exp(-1) = 0.6321$, the characteristic time to reach steady state is defined as the point in time when 63.21% of $c_{w,s-s}$ is achieved.

To evaluate if groundwater recharge or biodegradation, or both, are the decisive factors for the steady-state concentration levels, we use the Damköhler number (Damköhler, 1936), Da [−], which relates the time scale of flow ($t_a = h/q$) to the time scale of biodegradation ($t_r = 1/$):

$$Da = \frac{t_a}{t_r} = \frac{\lambda\theta h}{q}. \quad \text{(B7)}$$

The Da term is included in the denominator of Eq. (B6). If $Da \ll 1$, the long-term steady state is dominated by groundwater recharge, and the output concentration equals the input concentration; if $Da > 1$, the long-term steady state is dominated by both groundwater recharge and biodegradation and for $Da > 100$, biodegradation takes over.

Fig. B1 shows the comparison of our numerical model outcomes (symbols) accounting for all processes (advection, dispersion, diffusion, biodegradation and sorption) with the simple analytical solution for the box model (line, Eq. (B4)). In this case, $Da \approx 31$, which indicates that biodegradation is important. Except for small differences at early times (which is due to diffusion/dispersion not covered in the analytical solution), an excellent match of our numerical model results with the analytical solution is achieved. Furthermore, the characteristic time (Eq. (B6)), derived from the analytical solution, can be applied to estimate the time period needed to reach steady state.

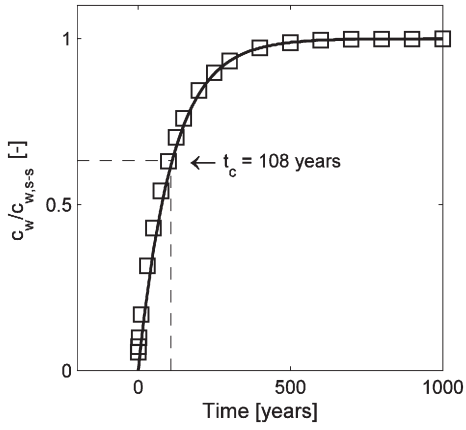

Fig. B1. Model comparison of MIN3P (symbols) with the analytical solution of a simplified one-box model (line) accounting only for recharge and biodegradation (Eq. (B4)). $c_w/c_{w,s-s}$ refers to the normalized concentration in the aqueous phase and values of the box model parameters applied are $h = 5$ m, $q = 200$ mm/year, $\theta = 0.33$, $\lambda = 1.2 \times 10^{-6}$/s and $K_d = 78.3$ L/kg, respectively.

References

Atanassova, I., Brümmer, G.W., 2004. Polycyclic aromatic hydrocarbons of anthropogenic and biopedogenic origin in a colluviated hydromorphic soil of Western Europe. Geoderma 120, 27–34.

Atkins, P.W., 1986. Physical chemistry. 3rd ed. Oxford University, New York.

Beyer, A., Mackay, D., Matthies, M., Wania, F., Webster, E., 2000. Assessing long-range transport potential of persistent organic pollutants. Environ. Sci. Technol. 34, 699–703.

BGR, R. Mittlere järhliche Grundwasserneubildung (Tafel 5.5). Bundesanstalt für Geowissenschaften und Rohstoffe (BGR) in Hannover Access time: Nov. 20, 2014. URL: www.bgr.bund.de.

Bidleman, T.F., Leone, A.D., 2004. Soil–air exchange of organochlorine pesticides in the Southern United States. Environ. Pollut. 128, 49–57.

Bozlaker, A., Muezzinoglu, A., Odabasi, M., 2008a. Atmospheric concentrations, dry deposition and air–soil exchange of polycyclic aromatic hydrocarbons (PAHs) in an industrial region in Turkey. J. Hazard. Mater. 153, 1093–1102.

Bozlaker, A., Odabasi, M., Muezzinoglu, A., 2008b. Dry deposition of soil–air exchange of polychlorinated biphenyls (PCBs) in an industrial area. Environ. Pollut. 156, 784–793.

Cabrerizo, A., Dachs, J., Moeckel, C., Ojeda, M.J., Caballero, G., Barcelo, D., et al., 2011. Ubiquitous net volatilization of polycyclic aromatic hydrocarbons from soils and parameters influencing their soil–air partitioning. Environ. Sci. Technol. 45, 4740–4747.

Carsel, R.F., Parrish, R.S., 1988. Developing joint probability distributions of soil water retention characteristics. Water Resour. Res. 24, 755–769.

Cousins, I.T., Beck, A.J., Jones, K.C., 1999a. A review of the processes involved in the exchange of semi-volatile organic compounds (SVOC) across the air–soil interface. Sci. Total Environ. 228, 5–24.

Cousins, I.T., Gevao, B., Jones, K.C., 1999b. Measuring and modelling the vertical distribution of semi-volatile organic compounds in soils. 1: PCB and PAH soil core data. Chemosphere 39, 2507–2518.

Cousins, I.T., Gevao, B., Jones, K.C., 1999c. Measuring and modelling the vertical distribution of semi-volatile organic compounds in soils. 2: Model development. Chemosphere 39, 2519–2534.

Damköhler, G., 1936. Einflüsse der Strömung, Diffusion und des Wärmeübergangs auf die Leistung von Reaktionsöfen. Z. Elektrochem. 42 (12), 846–862.

Deutscher Wetterdienst (DWD),). Temperatur: langjährige Mittelwerte 1981–2010. Deutscher Wetterdienst Access time: Nov. 20, 2014. URL: www.dwd.de.

Farrar, N.J., Harner, T., Shoeib, M., Sweetman, A., Jones, K.C., 2005. Field deployment of thin film passive air samplers for persistent organic pollutants: a study in the urban atmospheric boundary layer. Environ. Sci. Technol. 39, 42–48.

Foken, T., 2008. Micrometeorology. Springer-Verlag, Heidelberg, Germany.

Ghirardello, D., Morselli, M., Semplice, M., Di Guardo, A., 2010. A dynamic model of the fate of organic chemicals in a multilayered air/soil system: development and illustrative application. Environ. Sci. Technol. 44, 9010–9017.

Gocht, T., Grathwohl, P., 2004. Polyzyklische aromatische Kohlenwasserstoffe aus diffusen Quellen. Umweltwiss. Schadst. Forsch. 16, 245–254.

Gocht, T., Moldenhauer, K.M., Püttmann, W., 2001. Historical record of polycyclic aromatic hydrocarbons (PAH) and heavy metals in floodplain sediments from the Rhine River (Hessisches Ried, Germany). Appl. Geochem. 16, 1707–1721.

Gocht, T., Klemm, O., Grathwohl, P., 2007. Long-term atmospheric bulk deposition of polycyclic aromatic hydrocarbons (PAHs) in rural areas of Southern Germany. Atmos. Environ. 41, 1315–1327.

Gouin, T., Mackay, D., Webster, E., Wania, F., 2000. Screening chemicals for persistence in the environment. Environ. Sci. Technol. 34, 881–884.

Grathwohl, P., 1998. Diffusion in Natural Porous Media: Contaminant Transport, Sorption/Desorption and Dissolution Kinetics. Kluwer, Boston, Massachusetts.

Harner, T., Mackay, D., Jones, K.C., 1995. Model of the long-term exchange of PCBs between soil and the atmosphere in the southern U.K. Environ. Sci. Technol. 29, 1200–1209.

Hedman, J.E., 2008. Fate of Contaminants in Baltic Sea Sediment Ecosystems: The Role of Bioturbation (PhD Dissertation) Stockholm University, Stockholm.

Jamshidi, A., Hunter, S., Hazrati, S., Harrad, S., 2007. Concentrations of chiral signatures of polychlorinated biphenyls in outdoor and indoor air and soil in a major U.K. conurbation. Environ. Sci. Technol. 41, 2153–2158.

Karapanagioti, H.K., Kleineidam, S., Sabatini, D.A., Grathwohl, P., Ligouis, B., 2000. Impacts of heterogeneous organic matter on phenanthrene sorption: equilibrium and kinetic studies with aquifer material. Environ. Sci. Technol. 34, 406–414.

Kleineidam, S., Rügner, H., Ligouis, B., Grathwohl, P., 1999. Organic matter facies and equilibrium sorption of phenanthrene. Environ. Sci. Technol. 33, 1637–1644.

Kleineidam, S., Schüth, C., Grathwohl, P., 2002. Solubility-normalized combined adsorption-partitioning sorption isotherms for organic pollutants. Environ. Sci. Technol. 36, 4689–4697.

Kleineidam, S., Rügner, H., Grathwohl, P., 2004. Desorption kinetics of phenanthrene in aquifer material lacks hysteresis. Environ. Sci. Technol. 38, 4169–4175.

Komprda, J., Komprdova, K., Sanka, M., Mozny, M., Nizzetto, L., 2013. Influence of climate and land use change on spatially resolved volatilization of persistent organic pollutants (POPs) from background soils. Environ. Sci. Technol. 47, 7052–7059.

Krauss, M., Wilcke, W., Zech, W., 2000. Polycyclic aromatic hydrocarbons and polychlorinated biphenyls in forest soils: depth distribution as indicator of different rate. Environ. Pollut. 110, 79–88.

Kuntz, D., Grathwohl, P., 2009. Comparison of steady state and transient flow conditions on reactive transport of contaminants in the vadose zone. J. Hydrol. 369, 225–233.

Lang, C., Tao, S., Wang, X., Zhang, G., Li, J., Fu, J., 2007. Seasonal variation of polycyclic aromatic hydrocarbons (PAHs) in Pearl River Delta region, China. Atmos. Environ. 41, 8370–8379.

Lee, R.G.M., Hung, H., Mackay, D., Jones, K.C., 1998. Measurement and modeling of the diurnal cycling of atmospheric PCBs and PAHs. Environ. Sci. Technol. 32, 2172–2179.

Lima, A.L.C., Eglinton, T.I., Reddy, C.M., 2003. High-resolution record of pyrogenic polycyclic aromatic hydrocarbon deposition during the 20th century. Environ. Sci. Technol. 37, 53–61.

Liu, Y., Beckingham, B., Rügner, H., Li, Z., Ma, L., Schwientek, M., et al., 2013a. Comparison of sedimentary PAHs in the Rivers of Ammer (Germany) and Liangtan (China): differences between early- and newly industrialized countries. Environ. Sci. Technol. 47, 701–709.

Liu, L., Wu, F., Haderlein, S., Grathwohl, P., 2013b. Determination of the subcooled liquid solubilities of PAHs in partitioning batch experiments. Geosci. Front. 4, 123–126.

Lohmann, R., Breivik, K., Dachs, J., Muir, D., 2007. Global fate of POPs: current and future research directions. Environ. Pollut. 150, 150–165.

Lyman, W.L., Reehl, W.F., Rosenblatt, D.H. (Eds.), 1990. Handbook of Chemical Property Estimation Methods: Environmental Behavior of Organic Compounds, 2nd ed. Mc Graw — Hill, New York.

Mackay, D., 2010. Multimedia Environmental Models: The Fugacity Approach. 2nd ed. CRC Press, Florida, USA.

MacLeod, M., Scheringer, M., Podey, H., Jones, K.C., Hungerbuehler, K., 2007. The origin and significance of short-term variability of semivolatile contaminants in air. Environ. Sci. Technol. 41, 3249–3253.

Mayer, U.K., Frind, E.O., Blowes, D.W., 2002. Multicomponent reactive transport modeling in variably saturated porous media using a generalized formulation for kinetically controlled reactions. Water Resour. Res. 38, 1174.

McKelvie, J.R., Åslund, M.W., Celejewski, M.A., Simpson, A.J., Simpson, M.J., 2013. Reduction in the earthworm metabolomics response after phenanthrene exposure in soils with high soil organic carbon content. Environ. Pollut. 175, 75–81.

Meixner, F.X., Andreae, M.O., van Dijk, S.M., Gut, U.A., Rummel, U.K., Scheibe, M., Welling, M., 2003. Biosphere-atmosphere exchange of reactive trace gases in a primary rainforest ecosystem: studies on interlinking scales. Rep. Ser. Aerosol Sci. 62A, 269–274.

Meyer, T., Wania, F., Breivik, K., 2005. Illustrating sensitivity and uncertainty in environmental fate models using partitioning maps. Environ. Sci. Technol. 39, 3186–3196.

Moeckel, C., Nizzetto, L., Strandberg, B., Lindroth, A., Jones, K.C., 2009. Air-boreal forest transfer and processing of polychlorinated biphenyls. Environ. Sci. Technol. 43, 5282–5289.

Moldrup, P., Olesen, T., Gamst, J., Schjønning, P., Yamaguchi, T., Rolston, D.E., 2000. Predicting the gas diffusion coefficient in repacked soil water-induced linear reduction model. Soil Sci. Soc. Am. J. 64, 1588–1594.

Moldrup, P., Olesen, T., Komatsu, T., Schjønning, P., Rolston, D.E., 2001. Division S-1 — soil physics: tortuosity, diffusivity, and permeability in the soil liquid and gaseous phase. Soil Sci. Soc. Am. J. 65, 613–623.

Müller, G., Grimmer, G., Böhnke, H., 1977. Sedimentary record of heavy metals and polycyclic aromatic hydrocarbons in Lake Constance. Naturwissenschaften 64, 427–431.

Ogata, A., Banks, R.B., 1961. A solution of the differential equation of longitudinal dispersion in porous media. USGS Professional Paper, p. 411-A.

Panagos, P., Hiederer, P., Van Liedekerke, M., Rampa, F., 2013. Estimating soil organic carbon in Europe based on data collected through an European network. Ecol. Indic. 24, 439–450.

Prevedouros, K., Brorstrom-Lunden, E., Halsall, C.J., Jones, K.C., Lee, R.G.M., Sweetman, A.J., 2004. Seasonal and long-term trends in atmospheric PAH concentrations: evidence and implications. Environ. Pollut. 128, 17–27.

Razzaque, M.M., Grathwohl, P., 2008. Predicting organic carbon–water partitioning of hydrophobic organic chemicals in soils and sediments based on water solubility. Water Res. 42, 3775–3780.

Reichman, R., Wallach, R., Mahrer, Y., 2000a. A combined soil–atmosphere model for evaluating the fate of surface-applied pesticides. 1. Model development and verification. Environ. Sci. Technol. 34, 1313–1320.

Reichman, R., Mahrer, Y., Wallach, R., 2000b. A combined soil–atmosphere model for evaluating the fate of surface-applied pesticides. 2. The effect of varying environmental conditions. Environ. Sci. Technol. 34, 1321–1330.

Rügner, H., Kleineidam, S., Grathwohl, P., 1999. Long term sorption kinetics of phenanthrene in aquifer materials. Environ. Sci. Technol. 33, 1645–1651.

Sanders, G., Jones, K.C., Hamilton-Taylor, J., Dorr, H., 1993. Concentrations and deposition fluxes of polynuclear aromatic hydrocarbons and heavy metals in the dated sediments of a rural english lake. Environ. Toxicol. Chem. 12 (9), 1567–1581.

Schneider, A.R., Stapleton, H.M., Cornwell, J., Baker, J.E., 2001. Recent declines in PAH, PCB, and toxaphene levels in the Northern Great Lakes as determined from high resolution sediment cores. Environ. Sci. Technol. 35 (19), 3809–3815.

Scholtz, M.T., Bidleman, T.F., 2006. Modelling of the long term fate of pesticide residues in agricultural soils and their surface exchange with the atmosphere: Part 1. Model description and evaluation. Sci. Total Environ. 368, 823–838.

Scholtz, M.T., Bidleman, T.F., 2007. Modelling of the long term fate of pesticide residues in agricultural soils and their surface exchange with the atmosphere: Part 2. Projected long-term fate of pesticide residues. Sci. Total Environ. 377, 61–80.

Schuster, J.K., Gioia, R., Sweetman, A.J., Jones, K.C., 2010. Temporal trends and controlling factors for polychlorinated biphenyls in the UK atmosphere (1991–2008). Environ. Sci. Technol. 44, 8068–8074.

Schwarzenbach, R.P., Gschwend, P.M., Imboden, D.M., 2003. Environmental Organic Chemistry. 2nd ed. John Wiley & Sons Inc., New Jersey.

Simcik, M.F., Eisenreich, S.J., Golden, K.A., Liu, S., Lipiatou, E., Swackhamer, D.L., Long, D.T., 1996. Atmospheric loading of polycyclic aromatic hydrocarbons to Lake Michigan as recorded in the sediments. Environ. Sci. Technol. 30, 3039–3046.

Tao, S., Wang, Y., Wu, S., Liu, S., Dou, H., Liu, Y., et al., 2007. Vertical distribution of polycyclic aromatic hydrocarbons in atmospheric boundary layer of Beijing in winter. Atmos. Environ. 41, 9594–9602.

Tao, S., Liu, W., Li, Y., Yang, Y., Zuo, Q., Li, B., et al., 2008. Organochlorine pesticides contaminated surface soil as reemission source in the Haihe plain, China. Environ. Sci. Technol. 42, 8395–8400.

Totten, L.A., Stenchikov, G., Gigliotti, C.L., Lahoti, N., Eisenreich, S.J., 2006. Measurement and modeling of urban atmospheric PCB concentrations on a small (8 km) spatial scale. Atmos. Environ. 40, 7940–7952.
van Jaarsveld, J.A., van Pul, W.A.J., De Leeuw, F.A.A.M., 1997. Modelling transport and deposition of persistent organic pollutants in the European region. Atmos. Environ. 31, 1011–1024.
Verschueren, K., 1983. Handbook of Environmental Data on Organic Chemicals. 2nd ed. van Nostrand Reinhold Company Inc., New York.
Vikesøe, J., Thomsen, M., Carlsen, L., Johansen, E., 2002. Persistent Organic Pollutants in Soil, Sludge and Sediment: A Multianalytical Field Study of Selected Organic Chlorinated and Brominated Compounds. National Environmental Research Institute Denmark, Roskilde. Report no. 402.
Wang, G., Grathwohl, P., 2013. Isosteric heats of sorption and desorption of phenanthrene in soils and carbonaceous materials. Environ. Pollut. 175, 110–116.
Wang, G., Kleineidam, S., Grathwohl, P., 2007. Sorption/desorption reversibility of phenanthrene in soils and carbonaceous materials. Environ. Sci. Technol. 41, 1186–1193.
Wang, W., Simonich, S., Giri, B., Chang, Y., Zhang, Y., Jia, Y., et al., 2011. Atmospheric concentrations and air–soil gas exchange of polycyclic aromatic hydrocarbons (PAHs) in remote, rural village and urban areas of Beijing-Tianjin region, North China. Sci. Total Environ. 409, 2942–2950.
Wania, F., Dugani, C., 2003. Assessing the long-range transport potential of polybrominated diphenyl ethers: a comparison of four multimedia models. Environ. Toxicol. Chem. 22, 1252–1261.
Wania, F., Breivik, K., Persson, N.J., McLachlan, M.S., 2006. CoZMo-POP 2 — a fugacity-based dynamic multi-compartmental mass balance model of the fate of persistent organic pollutants. Environ. Model. Softw. 21, 868–884.
Webster, F., Mackay, D., Wania, F., 1998. Evaluating environmental persistence. Environ. Toxicol. Chem. 17, 2148–2158.
Wilcke, W., Zech, W., Kobza, J., 1996. PAH-pools in soils along a PAH-deposition gradient. Environ. Pollut. 92, 307–313.
Wild, S.R., Jones, K.C., 1995. Polynuclear aromatic hydrocarbons in the United Kingdom environment: a preliminary source inventory and budget. Environ. Pollut. 88, 91–108.
Zhang, Y., Deng, S., Liu, Y., Shen, G., Li, X., Cao, J., et al., 2011. A passive air sampler for characterizing the vertical concentration profile of gaseous phase polycyclic aromatic hydrocarbons in near soil surface air. Environ. Pollut. 159, 694–699.
Zhong, Y., Zhu, L., 2013. Distribution, input pathway and soil–air exchange of polycyclic aromatic hydrocarbons in Banshan Industry Park, China. Sci. Total Environ. 444, 177–182.